Geophysical Characterization of Candidate Rock Contacts Within Igarra Area, South-Western Nigeria

MUSLIM B. AMINU

Department of Earth Sciences, Faculty of Science, Adekunle Ajasin University, Akungba – Akoko, Ondo State, Nigeria.

Abstract- ***The aim of this paper is to present the application and interpretation of multi-method near surface geophysical surveys including electrical resistivity imaging, total-field ground magnetic prospecting and ground electrical conductivity surveying to delineate lateral rock contacts in Igarra area in Southwestern Nigeria, especially in locations of poor rock exposure. The multi-method technique has practical application in detecting fracture zones for groundwater resource development; besides, the usefulness in improving the placement of locations of rock contacts accurately on geological maps. In the Igarra area, the lateral lithologic contacts have resulted from the metamorphism and re-crystallisation of initial contacts between sedimentary rocks, and also from late-stage granitic intrusions into pre-existing meta-sediments. Three geophysical profiles were taken in the study area. The profiles traverse contacts involving a transition from metaconglomerate-to-intrusive granite and two re-crystallized and rotated sedimentary boundaries; a metaconglomerate-to-quartzite and a phyllite-to-metaconglomerate boundary. Each boundary type yielded consistent diagnostic ground electrical resistivity and total field magnetic anomalies indicative of either the presence of groundwater or magnetic mineral concentrations at the contacts. The metaconglomerate-to-quartzite contact presented an electrical conductivity anomaly. However, the metaconglomerate-to-intrusive granite and the phyllite-to-metaconglomerate boundary did not present any electrical conductivity anomaly. The delineated rock contacts are potential supplementary source of groundwater and possible locations for the concentration of valuable minerals in the Igarra area.***

Indexed Terms- ***Lithologic contacts, near surface geophysics, low aperture fractures, groundwater, Igarra Schist belt.***

I. INTRODUCTION

Geophysical surveys rely on contrasting physical properties to delineate changes in subsurface conditions of underlying rock units. Such physical properties include the density of the rocks, magnetic susceptibilities, electrical conductivity occasioned by the amount of electrically conductive minerals and water present within the rock voids (Booth *et al*., 2019; Pazzi *et al*., 2019). Frequently, the contrast in rock property is evident and detectible in the vertical dimension (i.e., depth-wise), such as traversing the weathered overburden to the fresh bedrock or the lateritic topsoil to the top of the weathering substrate in areas of deep weathering (Rizzo *et al*., 2004; Robineau *et al*., 2007; Aminu, 2015a, 2018). In the lateral dimension, fractures within basement rocks and transitions from clayey soils to sandy loams offer the best candidates for detection and delineation (Park and Roberts, 2003; Bufford *et al*., 2012; Aminu *et al*., 2014; Chavez *et al*., 2014). Lateral contacts between different bedrock lithologies are often difficult to detect. When they are not the result of the juxtaposition of lithologies against one another as a result of faulting, lithologic contacts within the bedrock result from two basic scenarios: 1) the intrusion of younger magmatic bodies into pre-existing bedrock lithologies and; 2) the metamorphosis and subsequent rotation of originally horizontal boundaries between sedimentary units. The challenge with imaging these boundaries is that they often involve the re-crystallisation of the initial rock interfaces. This creates a gradual transition from the properties of one lithology to the other and the geophysical response becomes smeared-over and subtle. It is, however, possible that such re-crystallisations create detectable boundaries, such as hornfelsic rock suites or chill zones which may contain small aperture fractures, and flexural slips along the lithologic boundary which have resulted from folding

of the initial rock units (Tanner, 1989). These fissures can encourage the flow of juvenile fluids and the precipitation of both magnetically or electrically conductive minerals in reasonable concentrations (Pirajno, 2009).

In this paper, observations from multi-method geophysical surveys across three categories of bedrock lithologic boundaries are presented; 1) a hornfelsic boundary resulting from the intrusion of a granitic rock into earlier metaconglomerates; 2) a metaconglomerate-quartzites contact blinded over by thin soil cover; and 3) a phyllite-metaconglomerate contact along which fractures have developed. We have established that by careful observation and interpretation, lithologic contacts/ boundaries can be detected using geophysical surveying.

Conventionally, geophysics tools are employed in the investigation of subsurface geologic structure for diverse reasons (LaBrecque *et al.*, 1996; Zume *et al.*, 2006; Frid *et al.*, 2007; Lines *et al.*, 2012; Aminu *et al.*, 2014, 2015a, b, 2018). The geophysical techniques provide non-invasive sensing of rock properties with a reasonable trade-off between cost and accuracy. Geophysics tools have found extensive use in groundwater prospecting (Zume *et al*., 2006; Frid *et al.*, 2012; Mohamed *et al*., 2012), in construction-site investigations (Soupios *et al*., 2002; El-Qady *et al*., 2005; Chavez *et al*., 2014; Yassin *et al*., 2014; Aminu, 2018), in mineral exploration (Hoover *et al*., 1992; Kataka *et al*., 2018), and in delineating bedrock morphology and spatial distribution of underlying geologic features (Aminu, 2015a). They are also useful in ground corrosivity studies (Ekwe *et al*., 2018), in quantitative estimation of in-situ geotechnical properties (Anderson, 2006; Cosenza *et al*., 2006), and in unravelling the tectonic history of surveyed areas (Bufford *et al*., 2012; Aminu *et al*., 2014).

Bufford *et al*. (2012) imaged the geometry and nature of fault activity along the Okavango Rift Zone in Botswana in the southwestern branch of the East African Rift System. The rift zone was delineated as a low resistivity path which was interpreted to channel both surface water and groundwater from the Okavango delta and re-circulating it through lacustrine and fluvio-deltaic sediments of the basin. El-Qady *et al*. (2005) employed ground-penetrating radar and electrical resistivity imaging to reveal the subsurface structure of a Karst cave over a proposed site for low-income residential apartments in the eastern parts of greater Cairo. Previously unknown extensions of the cave system were delineated as zones of marl, and multiple vertical fractures in limestones. Aminu *et al*. (2014) employed electrical resistivity imaging to delineate the Uneme-Nekhua fracture zone. The fracture zone was imaged as consisting of two distinct fractures where deformation had ceased on one fracture and had been transferred to the other. Park and Roberts (2003) utilize prior magnetotelluric (MT) data and electrical resistivity and formation factor data from core plugs of sedimentary rocks within the San Andreas Fault to offer an alternative interpretation of MT data presented in Unsworth *et al*. (1997). They averred that the anomalous region resulted from conductive sedimentary rocks within the plunging syncline adjacent to the fault rather than fractured rock.

II. GEOLOGICAL SETTING

The study area is located between Longitudes 05˚ 43˙E and 05 ˚ 47˙ E, and Latitudes 07˚ 27˙N and 07˚ 31˙N within Igarra area in the extreme north of Edo State, Nigeria, (Figure 1). The study area is within the Igarra schist belt of the Basement Complex of southwestern Nigeria, a region consisting of predominantly of migmatitic and granitic gneisses (Rahaman, 1989; Turner, 1989). The area consists of a westward sloping low lying area walled on the eastern side by a N-S trending granitic ridge which rises above the surrounding areas. Topographic relief is 345 m above sea-level and reaches up to 600 m on the top of the granitic ridge. Drainage is provided by a number of seasonal streams flowing from the high reliefs in the east and empty west of the town. The Igarra town is curved around the south-western end of the granitic ridge.

The Igarra area is characterized by an open synform which refolded in E-W folds. The mini-basin consists of metamorphosed calcareous rocks and conglomerates occurring along with quartzites as steeply dipping bands in the dominant biotite gneiss (Turner, 1989). Older migmatites form the periphery around the synform. The structural evolution of the

area began with crustal thinning (Figure 2) that led to the formation of a mini-basin which was filled by sediments obtained from the adjoining continental areas. A metamorphic episode and two deformation episodes led to re-crystallization, folding and refolding of the initial sedimentary pile and the development of abundant fractures. The next phase was followed by late-stage intrusives, mostly of mostly of porphyritic-granite and minor amount of aplite/

Fig. 1. Map of the study area (Google 2018). The Igarra Township curves around the south-western edge of the granitic ridge which blinds its eastern limits. Traverse locations are indicated in yellow discs. Dashed arrow lines (*not to scale*) indicate traverse orientation.

pegmatite, syenite, and subsidiary quartz vein. Subsequently, tectonic uplift and erosion exposed lateral alternations of metasedimentary rocks and their contacts with intrusive granites. Hornfelsic rocks are common at the contacts with intrusive granites. The geologic associations and structural development of the area have been discussed in details by Odeyemi (1988), Annor (1998) and Ogbe *et al*. (2018).

III. STUDY PROFILE SITES

Three profiles from three independent surveys were taken within the Igarra area (Figure 1). One profile straddled across a contact between host metaconglomerates and its granitic intrusive with hornfelsic textured rock at the contact. The contact is visible along a road-cut exposure on the Auchi-Ibillo expressway. The second profile was taken across a metaconglomerate-to-quartzite boundary which is covered by thin overburden. Metaconglomerate and quartzite outcrops are visible few metres away on either side of the inferred contact. The third profile straddled across the Orle river channel in the northern part of Igarra town. Along this profile, the channel is known to occur approximately along the lithologic contact between phyllites which outcrop few meters south of the river channel axis and metaconglomerates which outcrop few tens of metres north of the river channel.

IV. MATERIALS AND METHODS

A. Data Collection

The three (3) traverse locations in the study area are presented in Figure 1. The first traverse, T_1, has a total length of 100m and it straddled across a contact between a host metaconglomerate rock and its intrusive granitic guest. T_1 traverse is situated in a northwest-to-southeast direction along the southern shoulder of the Auchi-Ibillo road. The actual contact is marked by hornfelsic (burnt) rocks exposed by a road-cut adjacent to the northern shoulder of the road. The second traverse, T_2, is 100 m long and straddled across a contact between metaconglomerate and quartzite in a southwest-to-northeast direction. The T_2 contact is covered by relatively thin overburden and outcrops of metaconglomerate and quartzite can be seen not far from the inferred contact on both sides. The third traverse, T_3, is 200 m long and straddled across the fracture-controlled Orle river channel in a southeast-to-northwest trend. Phyllites outcrop less than 10 m south of the river channel and metaconglomerates can be seen at about 60 m on the northern side. Each of the three traverses is part of wider multiple surveys to characterize rock contacts in the study area. Data collected were 2D Electrical Resistivity, Total Magnetic Field Intensity, and Electrical Conductivity. Electrical resistivity data were collected using the ABEM 1000 Terrameter system. The dipole-dipole electrode array

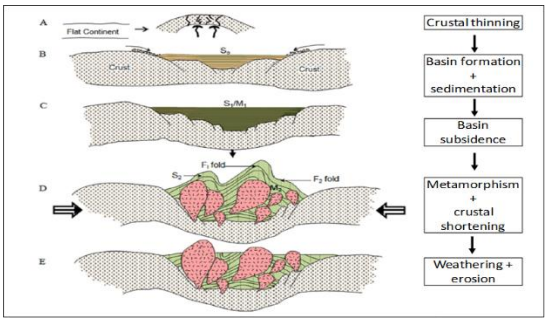

Fig. 2. Idealised model of the geological evolution of the Igarra area. Subsidence, sedimentation, metamorphism and associated folding and finally erosion have resulted in lateral lithologic contacts between metasediments and igneous intrusives (Modified after Ogbe *et al*., 2018).

was employed in all the surveys. Dipole spacing on T_1 and T_2 was 5 m and a maximum dipole length of 40 m was achieved on each traverse. On T_3, dipole spacing was maintained at 10 m and a maximum dipole length of 70 m was achieved. Total magnetic field intensity measurements were collected on all traverses using the GEMS System Magnetometer. Magnetic data were collected at 5 m spacing on all three traverses. Ground electrical conductivity data were collected at 5 m station spacing along all three traverses using the Geonics Coplanar loop EM34 system. A coil separation of 10 m was utilized. Data were collected in March 2017, just at the beginning of the rainy season.

A. Data Processing

Electrical resistivity data were de-spiked and data inversion was performed using DIPROfWIN 4.0.1, a 2.5D finite element modelling inversion algorithm (Yi and Kim, 1998). The program utilizes the Active Constraint Balancing scheme to determine the spatially varying Lagrangian multipliers for the least-squares inversion algorithm in a bid to optimize between robustness and smoothness of the inversion: an initial synthetic subsurface resistivity distribution model is computed and matched with the actual resistivity distribution, the difference between the two is reduced via an iterative process until a reasonable fit is achieved. Once the mismatch error drops below 5 %, the inversion is deemed suitable and the iteration is stopped. Three images were produced, namely: the observed field data pseudo-section, the computed theoretical data pseudo-section, and the inverted subsurface resistivity structure. Visual inspection of the observed field data pseudo-section distribution and the computed theoretical data pseudo-section further helped in the assessment of the robustness of the inversion. In this paper, a logarithmic colour display was utilized as the inverted resistivity range was wide (>20,000 Ohm-m). The display was limited to the range 89 - 6,000 Ohm-m as that provided the best visual representation of resistivity distributions along the traverses. Topographic variations were factored in during the inversion process for T_2 and T_3. The site for T_1 was flat. Total magnetic field intensity data were smoothened for spikes and reduced using a regional 32,500 nT background value. The resulting Residual Magnetic Intensity (RMI) values were presented along the traverses. Electrical conductivity measurements were simply plotted against station positions.

B. Interpretation Criteria

Interpretation criteria for resulting 2D subsurface resistivity structures of the subsurface of the study area is similar to those utilized by Aminu *et al*. (2014, 2015a, b). High laterally and or vertically continuous resistivities in the subsurface and at depth (usually above 1,500 Ohm-m) were interpreted to indicate unfractured bedrock. Low continuous-in-the-subsurface resistivities (usually below 150 Ohm-m) were interpreted to represent water-saturated surficial humus and clay-rich top-soil. Resistivities ranging from 160 - 1,500 Ohm-m were interpreted as partly weathered bedrock, conductive fracture paths or possibly lithologic contacts, depending on the lateral and vertical continuity and geometry of the imaged responses. Inflection points on magnetic measurements and conductivity lows were interpreted as possible fracture zones or rock contacts. Rock contacts are weak zone with the potential to host fractures. Magnetic and electrically conductive minerals can accumulate along these fractures when hydrothermal fluids and groundwater flow through them (Pirajno, 2009). Further, interpretations of the geophysical responses from all data were constrained by the geological information afforded by the geological setting and rock outcrops within the area.

V. RESULTS

Figure 3 is a panel consisting of plots of the inverted 2D subsurface resistivity response beneath T_1 and the corresponding residual magnetic intensity and electrical conductivity responses. T_1 traverse is oriented in northwest-to-southeast direction. High resistivity responses (>1,500 Ohm-m) are continuous at depth along the profile. The upper limit of this response is undulating and shallow in the southeastern half of the traverse at roughly 3 - 4 m below the ground surface. In the northwestern half, the depth to this high resistivity

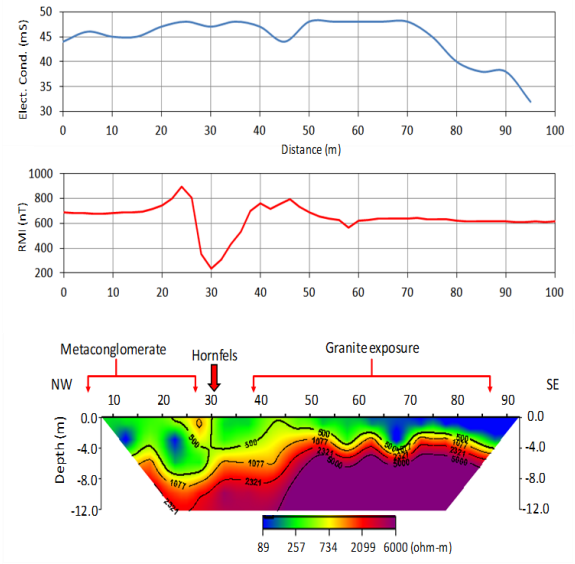

Fig. 3. Composite panel of 2D subsurface resistivity image, residual magnetic intensity, and ground electrical conductivity response along traverse 1. The metaconglomerate-granite contact is marked by lower resistivity responses, deeper weathering profile and a distinct magnetic anomaly at about the 30 m marks.

response reaches 8 - 12 m. Very low resistivity response patterns (<150 Ohm-m) occur in the near-surface 2 - 3 m of the traverse in the southeastern half of the traverse and caps and fills troughs atop the high resistivity responses. Intermediate resistivity (160 - 1,500 Ohm-m) patterns occur from the ground surface to depths of 5 - 10 m in the northwestern half of the traverse. An asymmetric residual magnetic anomaly occurs at about 25 - 35 m along the traverse. The magnetic anomaly roughly coincides with the location of hornfels along the traverse. The conductivity plot is flat at 44 - 48 mS almost all through the traverse. The exception is in the southeastern end where conductivity drops off to 32 mS.

Figure 4 is a panel consisting of plots of the inverted 2D subsurface resistivity response beneath T_2 and the corresponding residual magnetic intensity and electrical conductivity responses. This traverse is oriented in the southwest-to-northeast direction. High resistivity responses (>1,500 Ohm-m) occur at depth from the southwestern end of the traverse till roughly the 50 m position. The upper surface of the response occurrs at an average depth of 3 m below the ground surface with an undulating topology. The pattern coincides with the area with numerous metaconglomerate rock outcrops occur. A second, high resistivity pattern, occurs at 65 - 85 m along the traverse and coincides with a region of outcropping quartzites. These two high resistivity patterns are separated by an intervening intermediate resistivity pattern (160 - 1,500 Ohm-m) that extends from an average depth of 3 m beneath the ground surface at 45 – 65 m. The intermediate pattern appears to dip in the northeast direction at a high angel of ~60˚. The residual magnetic plot bears a magnetic low at 25 – 40 m within outcropping metaconglomerates. Electrical conductivity is generally low (15 mS) but has a clear negative signature at 40 - 60 m.

Figure 5 is a panel consisting of plots of the inverted 2D subsurface resistivity response beneath T_3 and the corresponding residual magnetic intensity and electrical conductivity responses. The traverse was oriented in the southeast-to-northwest direction.

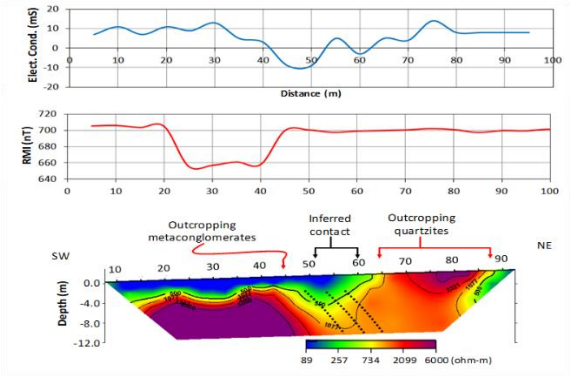

Fig. 4. Composite panel of 2D subsurface resistivity image, residual magnetic intensity, and ground electrical conductivity response along traverse 2. The inferred contact is coincident with lower bedrock resistivities and a low ground electrical conductivity anomaly while also roughly northwards of a distinct magnetic anomaly. The contact possibly dips northeast at high angles and may host fractures in the bedrock (Black dashed lines).

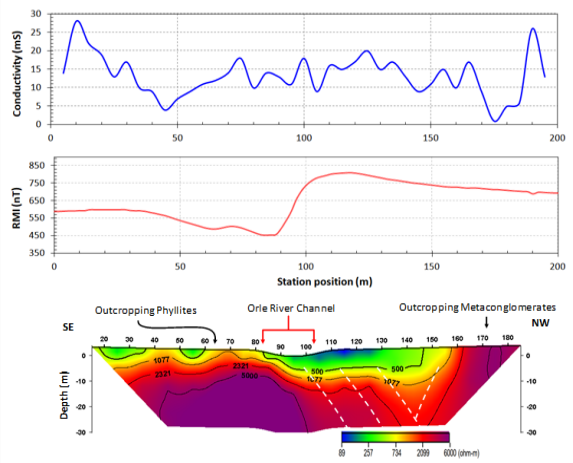

Fig. 5. Composite panel of 2D subsurface resistivity image, residual magnetic intensity, and ground electrical conductivity response along traverse 1. The contact region coincides with low bedrock resistivity and an asymmetric magnetic anomaly. It appears wide (100 – 150 m) and hosts fractures (white dashed lines) some of which are visible in rock at the channel bottom in the dry season.

The resistivity response consists of three patterns. The first response pattern had high resistivity responses (>1,500 Ohm-m) that occurred continuously at depth nearly all through the section. Generally, the upper limits of the high response patterns occur at 2 - 4 m depth. However, the pattern nearly reached the surface at 40 - 50 m and 60 - 70 m. In the northern extremes of the traverse, the pattern reached the surface. Phyllite outcrops were found in the west of T_3 traverse at the 60 - 70 m mark. Low-lying metaconglomerate outcrops were found in the East of the northern end of the traverse. The upper limit of the pattern also forms a trough between 80 m and 150 m. Beneath the trough region, much lower resistivity responses occur and appear to separate the high resistivity response pattern into two segments. Low resistivity responses (<150 ohm-m) occur at the surface at 90 - 130 m reaching a maximum depth of ~ 6 m. The pattern sits within the trough on the upper limit of the high resistivity pattern and is largely coincident with the Orle river channel at 85 - 105 m. On T_3 traverse, intermediate resistivity responses (160 - 1,500 Ohm-m) occur in the near-surface of the southern end of the traverse (18 - 36 m and 50 - 60 m) and as a generally thin layer underlying the low resistivity responses within the trough region. They separate the high resistivity and low resistivity responses. Between 120 - 160 m, the pattern extends to depths greater than 20 m and appears to separate the high resistivity response pattern into southern and northern segments. The residual magnetic anomaly is positive along the traverse and shows as a distinct asymmetric magnetic anomaly in the middle of the traverse (90 - 100 m). The inflection point on the anomaly is approximately coincident with the location of Orle river channel. The conductivity response oscillates in no systematic pattern from 1 - 28 mS.

VI. DISCUSSION

The panels presented in the result section describe the geophysical responses across three distinct lithologic contact types: Type 1, a metaconglomerate-granite contact that resulted from the intrusion of late-stage granites into pre-existing metaconglomerate (Figure 3); Type 2, is a metaconglomerate-quartzite contact that resulted from the co-metamorphoses of the individual parent sedimentary rocks (conglomerate and sand-rich sandstones), then the original sediment interface was re-crystallized and rotated to the vertical plane by folding, and Type 3, a phyllite-metaconglomerate contact that was formed in similar fashion to the metaconglomerate-quartzite contact and which subsequently had experienced extensive fracturing. These lithologic contacts are different from conventional along-fault juxtaposition of rocks which generally have wider aperture deformation zones (fault zone) that have been well imaged in literature (Unsworth, 1997; Park and Roberts, 2003). In contrast, lithologic contacts are low aperture zones which may host chill-zones and hornfels such as when resulting from intrusives (Types 1), or which may host flexural slips along contact lines during subsequent folding episodes (Types 2), and even low aperture fractures (Types 3).

The metaconglomerate-granite contact (Figure 3) presented with two distinct geophysical signatures; the subsurface electrical resistivity response increased significantly (from intermediate resistivities [160 - 1,500 Ohm-m] to >1,500 Ohm) in traversing the contact from metaconglomerate to granite. Further, overburden development is deeper on the region of the pre-existing metaconglomerates (up to 8 m deep) in contrast to shallow development in the region with granites (averagely 3 m). A clear magnetic anomaly

also coincided with the outcrop location of hornfels (burnt rock) between the two lithologies. No electrical conductivity anomaly was identified on the contact. In the metaconglomerate-quartzite contact (Figure 4), the inferred contact was characterized also by distinct geophysical signatures: 1) the subsurface electrical resistivity response at the inferred contact was much lower for depths in excess of 4 m compared to either side of the contact. The contact zone appears to be about 8 m wide and has an apparent dip of roughly 60˚ in the northeast direction. A low electrical conductivity anomaly was also largely coincident with the inferred contact. A magnetic low overlies the region with outcropping metaconglomerates approximately 10 m southwest of the inferred contact. It is possible, though challenging, to ascribe this magnetic anomaly to the inferred contact. It is plausible that the contact involves flexural-slip or fracturing resulting from the folding episodes which deformed and rotated the boundary. The Phyllite-metaconglomerate contact (Figure 5) also presented two clear geophysical anomalies: (1) Subsurface resistivity response beneath the channel-pass was much lower (intermediate resistivities – 1,000 - 1,500 Ohm-m) compared to the rest of the section for depths greater than 6 m. The area is about 50 m wide (spanning 100 – 150 m along the traverse). Multiple fractures were inferred within the area with a few visible at the bottom of the Orle river channel during the dry season when the river volume is low. (2) An asymmetric magnetic anomaly that coincided with the location of the Orle river channel in the southeastern section of the lowered resistivity anomaly. The anomaly shape is indicative of a fracture with a northwest dip.

The electrical resistivity and total field magnetic survey methods offered the most consistent and robust diagnostic anomalies over the lithologic contact zones in all the three cases. That consistence possibly resulted from the development of fractures and flexural slips along the contacts which subsequently allowed the flow of either groundwater or late-stage magmatic fluids through the rocks. Those two processes lowered the electrical properties of the contact zones thereby making them detectible. They also present the potential to concentrate magnetic minerals along those zones either through wall-rock mineral alterations or via the deposition of magnetic minerals by magmatic fluids (Pirajno, 2009). Although ground electrical conductivity surveys respond to both lowered resistivity (inverse of conductivity) resulting from the presence of water in fractures and higher electrical conductivity due to the presence of magnetic and conductive minerals, its failure to consistently detect the contacts in this study possibly resulted from the relative low aperture-size of the contacts in comparison to the special resolution of the coil spacing employed.

CONCLUSION

In this paper, three geophysical traverses involving the application of 2D electrical resistivity imaging, total field magnetic and ground conductivity data were utilised to identify candidate rock contacts within Igarra area. The contacts between host metaconglomerate and intrusive granites, and metamorphosed metaconglomerate-quartzite and phyllite-metaconglomerate boundaries have low aperture fissures compared to major faulted structures. The contacts consistently indicated electrical resistivity anomalies; as a zone of deep-weathering at hornfelsic rocks at the metaconglomerate-granite contact and as a vertical to near-vertical lower resistivity structures in the imaged bedrock in the metaconglomerate-quartzite and phyllite-metaconglomerate contacts. Magnetic anomalies are associated with all three contact types. Only the metaconglomerate-quartzite contact show identifiable ground electrical conductivity anomaly. This study indicates that by applying multi-method geophysical surveys and careful interpretation, rock contacts can be delineated with a high level of certainty. This is important as rock contacts may contain narrow aperture fracture zones and flexural slip which may serve to channel groundwater or host valuable mineral resources. The results further established that careful applications of near surface geophysical prospecting can aid the determination of lithologic boundaries in areas of poor rock exposure. This can be useful in improving the placement of lithologic contacts of geological maps.

ACKNOWLEDGMENT

The author wishes to acknowledge the Tertiary Education Trust Fund of the Federal Republic of

Nigeria for support under the Institution Based Research Initiative (VC/APU/025). The author further acknowledges Adedibu Sunny, Adekunle Sadiq, and Mufutau Isiaka for field support.

REFERENCES

[1] Aminu, M. B., Akande, T. M. and Ishola, A. O. -2D Geoelectric Imaging of the Uneme-Nekhua Fracture Zone. *International Journal of Geophysics*, 2014. http://dx.doi.org/10.1155/2014/842812

[2] Aminu, M. B. -Electrical Resistivity Imaging of a Thin Clayey Aquitard Developed on Basement Rocks in Parts of Adekunle Ajasin University Campus, Akungba-Akoko, South-western Nigeria. *Environmental Research, Engineering and Management*, vol. 71, no. 1, pp. 47-55. 2015a.

[3] Aminu, M. B. -Geo-electric Investigation of the Cause of Structural Failure Indices on a Set of Administrative Blocks. *Journal of Applied Geology and Geophysics*, vol. 3, no. 4, pp. 1-10, 2015b.

[4] Aminu, M. B. -Subsurface Electrical Resistivity Imaging and Electromagnetic Conductivity Profiling at a Proposed Construction Site at Adekunle Ajasin University Campus, Akungba-Akoko, South-Western Nigeria. *Global Journal of Geological Sciences*, vol. 16, pp. 53-60, 2018.

[5] Annor A.E. -Structural and Chronological relationship between the low grade Igarra Schist and adjoining Okene Migmatite-Gneiss terrain in the Precambrian exposure of Southwestern Nigeria. *Journal of Mining and Geology*, vol. 34, pp. 194-97, 1998.

[6] Anderson, N. L. -Selection of Appropriate Geophysical Techniques: A Generalized Protocol Based on Engineering Objectives and Site Characteristics. Proc., 2006 Highway NDE Conference, 2006, pp. 29-47. http://2006geophysics.mst.edu/.

[7] Booth, A. D., Vandeginste, V., Pike, D., Abbey, R., Clark, R. A., Green, C. M. and Howland, N. -Geochemical constraints in near-surface geophysical surveying from in situ XRF spectrometry: Field trials at two aviation archaeology sites. *In*: Persico, R., Piro, S. and Linford, N. (Eds). Innovation in Near-Surface Geophysics: Instrumentation, Application, and Data Processing Methods. Elsevier, 2019, pp. 97-119.

[8] Bufford, K. M., Atekwana, E. A. and Abdelsalam, M. G. -Geometry and faults tectonic activity of the Okavango Rift Zone, Botswana: evidence from magnetotelluric and electrical resistivity tomography imaging. *Journal of African Earth Sciences*, vol. 65, pp. 61-71, 2012.

[9] Chavez, R. E., Cifuentes-Nava, G., Tejero, A., Hernandez-Quintero, J. E., and Vargas, D. -Special 3D electric resistivity tomography (ERT) array applied to detect buried fractures on urban areas: San Antonio Tecomitl, Milpa Alta, Mexico. *Geofisica Internacional* vol. 53, no. 4, pp. 425-434, 2014.

[10] Cosenza, P., Marmet, E., Rejiba, F., Cui, Y. J., Tabbagh, A., and Charlery, Y. -Correlations between geotechnical and electrical data: A case study at Garchy in France, *Journal of Applied Geophysics*, vol. 60, no. 3, pp. 165-178, 2006.

[11] El-Qady, G., Hafez, M., Abdalla, M. A. and Ushijima, K. -Imaging subsurface cavities using geoelectric tomography and ground penetrating radar, *Journal of Cave and Karst Studies*, vol, 67, no. 3, pp. 174-181, 2005.

[12] Ekwe, A., Opara, A. and Onwuka, O. -Geoelectrical study of corrosivity and competence of soils within Uburu and Okposi areas of Ebonyi State, Southeastern Nigeria. *Anti-Corrosion Methods and Materials*, vol. 65, no. 6, pp. 637-645, 2018.

[13] Frid, V., Liskevich, G., Doudkinski, D. and Korostishevsky, N. -Evaluation of landfill disposal boundary by means of electrical resistivity imaging. *Environmental Geology*, vol. 53, no. 7, pp. 1503-1508, 2008.

[14] Hoover, D.B., Heran, W.D., and Hill, P.L., eds., The geophysical expression of selected mineral deposit models: *U.S. Geological Survey Open-file Report 92-557*, 1992, 129 p.

[15] Kataka, M. O., Mundalamo R. H., Ratshiedena P. E. and Nemasea, T. -Application of geophysical techniques in mineral exploration for potential sulphide deposits in Musina area 5th International

Conference on Geological and Environmental Sustainability, August 13-14, 2018, Bali, Indonesia. DOI: 10.4172/2381-8719-C1-017

[16] LaBrecque, D. J., Ramirez, A. L., Daily, W, D., Binley, A. M. and Schima, S. A. -ERT monitoring of environmental remediation processes," *Measurement Science and Technology*, vol. 7, no. 3, pp. 375-383, 1996.

[17] Lines, J. P., Bernardes, S., He, J., Zhang, S., Bacchus, S. T., Madden, M., and Jordan, T. -Preferential Groundwater Flow Pathways and Hydroperiod Alterations Indicated by Georectified Lineaments and Sinkholes at Proposed Karst Nuclear Power Plant and Mine Sites. *Journal of Sustainable Development*, vol. 5, no. 12, pp. 78-116, 2012.

[18] Mohamed, N. E., Brasse, H., Abdelgalil1, M. Y. And Kheiralla, K. M. -Geoelectric and VLF electromagnetic survey on complex aquifer structures, Central Sudan. *Comunicacoes Geologicas* vol. 99, no. 2, pp. 95-100, 2012.

[19] Odeyemi I. B. -Lithostratigrahic and structural relationship of the upper Precambrian metasediments of the Igarra area, Southwestern Nigeria. In: Oluyide, P.O., Mbonu, W.C., Ogezi, A.E., Egbunike, I.G., Ajibade, A.C., Ana-Umeji, A.C. (Eds.) Precambrian geology of Nigeria. Geological Survey Nigeria Publication, Kaduna, 1988, pp. 111-123.

[20] Ogbe, O. B., Olobaniyi, S.B., Ejeh, O. I., Omo-Irabor, O. O., Osokpor, J., Ocheli, A., Overare, B. -Petrological and structural investigation of rocks around Igarra, Southwestern Nigeria. *Ife Journal of Sciences*, vol. 20, no. 3, pp. 663-677, 2018.

[21] Park, S. K. and Roberts, J. J. -Conductivity structure of the San Andreas fault, Parkfield, revisited. *Geophysical Research Letters, vol. 30, no. 16*, pp. 1842, 2003. doi:10.1029/2003GL017689, 2003.

[22] Pazzi, V., Morelli, S. and Fanti, R. -A Review of the Advantages and Limitations of Geophysical Investigations in Landslide Studies. *International Journal of Geophysics*. 2019. doi.org/10.1155/2019/2983087

[23] Pirajno, F. -Hydrothermal Processes and Wall Rock Alteration. In: Hydrothermal Processes and Mineral Systems. Springer, Dordrecht, 2009, pp. 73-164.

[24] Rahaman, M. A. -Review of the Basement Geology of South-Western Nigeria. In: C. A. Kogbe (Ed), Geology of Nigeria, Nigeria: Rock View Limited), 1989, pp. 39-56.

[25] Rizzo, E., Colella, A., Lapenna, V. and Piscitelli, S. -Highresolution images of the fault-controlled High Agri Valley basin (Southern Italy) with deep and shallow electrical resistivity tomographies. *Physics and Chemistry of the Earth*, vol. 29, no. 4, pp. 321-327, 2004.

[26] Robineau, B., Join, J. L., Beauvais, A., Parisot, J-C. and Savin, C. -Geoelectrical imaging of a thick regolith developed on ultramafic rocks: groundwater influence," *Australian Journal of Earth Sciences*, vol. 54, no. 5, pp. 773-781, 2007

[27] Soupios, P. M., Georgakopoulos. P., Papadopoulos, N., Saltas, V., Andreadakis, A., Vallianatos, F., Sarris, A., and Makris, J. P. -Use of engineering geophysics to investigate a site for a building foundation, *Journal of Geophysics and Engineering*, vol. 4, no. 1, pp. 94-103, 2007.

[28] Tanner P.W. G. -The flexural-slip mechanism. *Journal of Structural Geology*. Vol. 11, no 6, pp. 635-655, 1989. ISSN 0191-8141.

[29] Turner, D. C. -Upper Proterozoic Schist Belts in the Nigerian Sector of the Pan-African Province of West Africa. In: C. A. Kogbe (Ed), Geology of Nigeria, Nigeria: Rock View Limited), 1989, pp. 93-109.

[30] Unsworth, M. J., Malin, P. E., Egbert, G. D. and Booker, J. R. -Internal structure of the San Andreas fault at Parkfield, California, *Geology*, vol. 25, pp. 359-362. 1997

[31] Yassin, R. R., Muhammad, R. F., Taib, S. H., and Al- Kouri, O., (). Application of ERT and Aerial Photographs Techniques to Identify the Consequences of Sinkholes Hazards in Constructing Housing Complexes Sites over Karstic Carbonate Bedrock in Perak, Peninsular Malaysia. *Journal of Geography and Geology*, vol. 6, no. 3, pp. 55-89. 2014.

[32] Yi, M. J., and Kim, J. H. -Enhancing the resolving power of the least squares inversion with Active Constraint Balancing: SEG

Expanded Abstracts, 68 Annual Meeting, New Orleans, 1998, pp. 485-488.

[33] Zume, J. T., Tarhule, A. and Christenson, S. - Subsurface imaging of an abandoned solid waste landfill site in Norman, Oklahoma. *Groundwater Monitoring and Remediation*, vol. 26, no. 2, pp. 62-69, 2006.